Effects of particle volume and shape on saltation motion of single particle in a turbulent flow over roughened bed

Yuya Takakuwa[1*], Shoji Fukuoka[1]

[1] Research and Development Initiative, Chuo University, 1-13-27 Kasuga, Bunkyo-ku, Tokyo 112-8551, Japan.

*Corresponding author. Tel.: +81 3 3817-1617. E-mail address: ytakakuwa099@g.chuo-u.ac.jp

Key Words: *Non-spherical particle, Movement manner, Instantaneous particle velocity, Fluid forces and collision forces, the APM method*

1. Introduction

Motions of particles in a turbulent flow over a roughened bed are controlled by hydraulic conditions, particle properties (physical properties, volume, and shape), bed roughness, particle-particle interactions, and fluid-particle interactions. We have assumed in previous sediment transport studies that the particle shape is spherical. However, effects of the particle shape cannot be neglected when dealing with large size particles, such as in bed variations in gravel-bed rivers. Effects of the particle shape on saltation motions have been investigated by focusing on the time-averaged particle velocity and hop length and height [1],[2], and there are few investigations about instantaneous particle velocity and forces acting on a moving particle. The Arbitrary Particle Multiphase method (the APM method [3]), a kind of Resolved CFD-DEM, is an effective method to solve these problems. Takakuwa and Fukuoka [4] performed the APM numerical simulations on saltation motion experiments [5] of single natural gravel with different volumes and shapes, and showed that the APM method can explain the transport process and the instantaneous velocity of non-spherical particles.

In this paper, effects of volume and shape on moving particle are clarified from time-averaged and instantaneous particle velocity, and fluid and collision forces of saltation motions of 12 particles with different volumes and shapes.

2. Computational setup and numerical scheme

As shown in Fig.1, a steady flow discharge 0.5 m^3/s is supplied from the upstream end (x = 0.0 m) of a straight channel with 45 m length, 1.08 m width and 1/20 bed slope, and a single particle is gently dropped from a height of 40 cm at x = 2.5 m, which follows the Shigemura's experiment [5]. The cross-sectional shape of the channel is designed to be a parabola, where particles tend to concentrate in the center of the channel. The channel bed was uneven due to the abrasion because the main aim of the Shigemura's experiment was understanding of abrasion mechanism of the channel bed by moving particles. The roughness at the bed is set by trial and error by superposing small spheres to reproduce the depth $\tilde{\bar{h}}^{Exp.}$ and the water surface velocity $\tilde{\tilde{u}}_s^{Exp.}$ measured by the Shigemura's experiment. The velocity distribution at x = 1.5 m is given at the upstream end in every time step to make the boundary

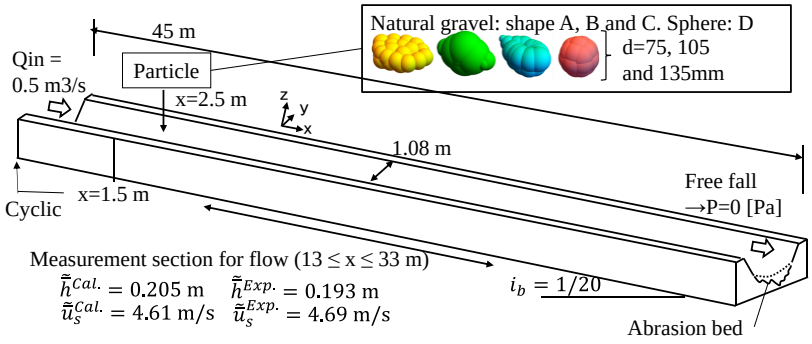

Figure. 1 Overview of numerical simulations.

Table. 1 Particle shapes. "a, b, and c" denote the longest, intermediate, and shortest axes, respectively. Dimensionless maximum projected area PA*max is the maximum projected area of the particle divided by that of the sphere with equivalent volume.

Shape name	a/d	b/d	c/d	Shape Factor = c/(ab)^0.5	Zingg's shape type	PA^*_{max}
A [6]	1.50	1.00	0.60	0.49	Disk	1.61
B [6]	1.39	1.01	0.79	0.67	Massive and symmetric	1.21
C [6]	1.34	0.90	0.83	0.76	Massive and asymmetric	1.25
D: Sphere	1.01	0.99	0.99	0.99	Massive	1.02

layer develop in the short distance. At the downstream end, a zero pressure is given for the free-fall flow in the experiment. 12 particles are used, consisting of 3 sizes (d = 75, 105, and 135 mm) and 4 shapes (see Fig.1 and Tab. 1. Natural gravel [5]: A Disk type, B Massive and symmetric type, C Massive and asymmetric type. D Sphere type). In this study, the particles are named by denoting their shapes and sizes, such as "A105".

The APM method [3] is a one of a Euler-Lagrange solvers. The fluid forces acting on an arbitrary shaped particle are directly calculated by detailed flows evaluated using a computational grid that is sufficiently smaller than a particle. Point collisions and areal contacts between particles and channel boundaries are evaluated by applying the Distinct Element Method (the Voigt model) to each small sphere making up a particle and a channel bed. Physical and numerical parameters are shown in Tab. 2.

Tab. 3 shows flow and channel characteristics. Fig.2 demonstrates time-averaged flow structures at x = 22.5 m. A high velocity of about 3.7 m/s is calculated at the channel center (y = 0.0 m), 0.05 m above the bottom, and secondary flows of Prandtl's second kind are also calculated in the corner between the bottom and the sidewall.

Table. 2 Physical and numerical parameters.

Density of fluid	1000	kg/m3
Density of particle	2500	kg/m3
Fluid viscosity	0.0010	kg/(m s)
Elastic modules	5.0E+10	Pa
Poisson's ratio	0.23	-
Coefficient of restitution	0.30	-
Coefficient of friction	0.20	-
Grid size	0.008	m
Number of grids (Nx*Ny*Nz)	5.7E+07 (=5629*147*69)	-
Time step for fluid calculation	2.0E-04	s
Time step for paritcle calculation	2.0E-06	s

Table. 3 Flow and channel characteristics at the channel center (y = 0.0 m).

Equivalent roughness	0.023	m
Depth	0.205	m
Depth-averaged velocity	3.88	m/s
Friction velocity	0.32	m/s
Froude number	2.73	-
Bulk Reynolds number	7.96E+05	-
Friction Reynolds number	6.53E+04	-
Shields number (d = 0.075, 0.105, 0.135)	0.092, 0.066, 0.051	-
d/ks (d = 0.075, 0.105, 0.135)	3.26, 4.57, 5.87	-

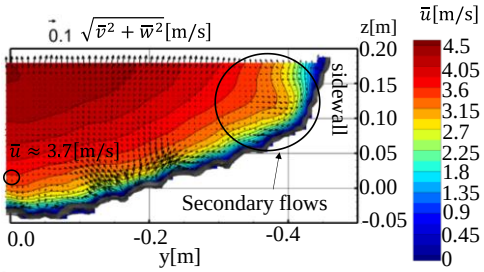

Figure. 2 Time-averaged flow structures at x = 22.5 m.

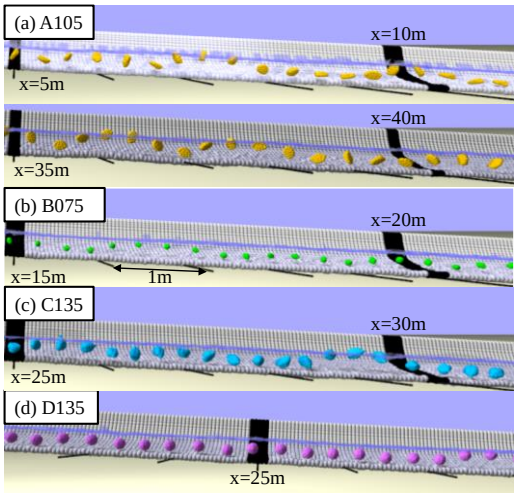

Figure. 3 Trajectories of A105, B075, C135 and D135 every 0.1 second.

3. Results and Discussions

First, characteristics of movement manners of each non-spherical particle are examined. As shown in Fig. 3(a), A105 moves in saltation with the longest or intermediate axis as the rotation axis and in rolling and saltation with the shortest axis as the rotation axis. Massive typed particles (B075 and C135) basically move by rolling or saltation with the longest axis as the rotation axis (Figs. 3(b) and (c)). However, C135, which has a strongly asymmetrical shape, has an unstable rotation, and sometimes leaps greatly after the angular point hits the roughened channel bed. The movement manners of these 3 particles found in the numerical simulations are similar to those of each particle in the Shigemura's experiment. The spherical particle (D135) simply rolls and jumps repeatedly (Fig. 3(d)). Under the conditions of these simulations, each particle is transported in the manner corresponding to its shape regardless of the particle size.

Second, the posture of non-spherical particles is investigated when particles are transported in their characteristic movement manners. Probability density distributions of the projected area of the non-spherical particles in the flow direction are compared (see Fig. 4). When disk typed (A) particles roll or jump with the shortest axis as the rotation axis, probability density distributions are different from the others, but the projected area of the other non-spherical particles in

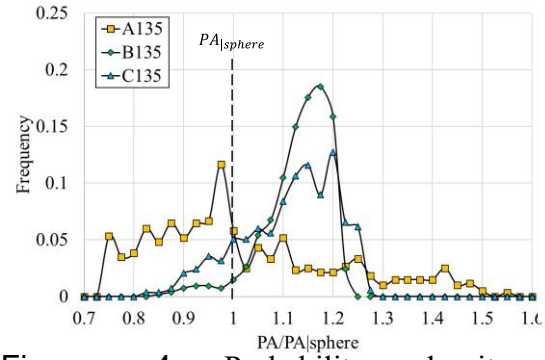

Figure. 4 Probability density distributions of the longitudinal component of the projected area of each non-spherical particle (d = 135 mm).

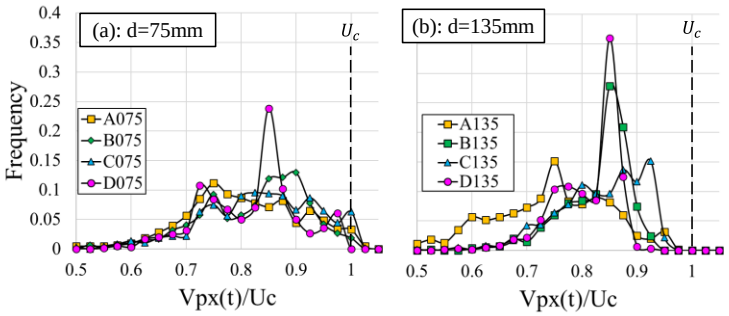

Figure. 5 Probability density distributions of the longitudinal component of the instantaneous particle velocity (Vpx(t)).

Table. 4 Time-averaged particle velocity.

	$\bar{V}_{px}$ [m/s]		
	75mm	105mm	135mm
A: Disk type	3.07	3.13	2.78
B: Massive and symmetric	3.15	3.18	3.16
C: Massive and asymmetric	3.19	3.18	3.18
D: Sphere	3.12	3.22	3.10

The depth averaged velocity (Uc) is 3.88 m/s.

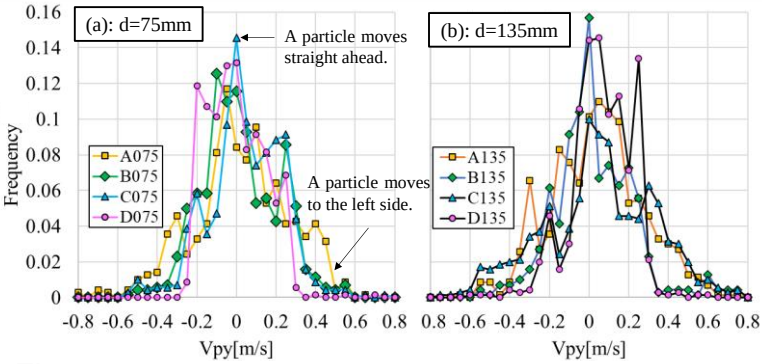

Figure. 6 Probability density distributions of the transverse component of the instantaneous particle velocity (Vpy(t)).

motion are basically larger than that of the sphere with the equivalent volume. This is different from the numerical result of Jain et al. [6] about bedload motions with various shapes over the fixed rough bed. In their numerical simulations, the particle-roughness ratio d/k_s and the Shields number Sh are small about 1.0 and 0.047, respectively, and non-spherical particles roll by interlocking with bed roughness (so called the engagement effect). On the other hand, the particle-roughness ratio and the Shields number in the present simulations are d/k_s (=3.26 ~ 5.87) and Sh (=0.051 ~ 0.092), and the saltation motion is dominant. It is considered that the particle movement postures are affected by these two parameters (d/k_s and Sh) whose values are greatly different in Jain's and our simulations.

Third, effects of particle volume and shape on the particle velocity are investigated. Except for A135, which frequently jumps higher than the water surface, the variation of the longitudinal component of the time-averaged particle velocity ($\bar{V}_{px}$) is very small, at most 4.7 %, as shown in Tab.4. It is also found that there are almost no effect of particle shape on the time-averaged velocity of a particle transported by flows with large Froud number, as shown in the results of previous studies [1] and [2].

In contrast, probability density distributions of the longitudinal component of the instantaneous particle velocity ($V_{px}(t)$) vary greatly depending on the particle volume and shape (see Fig. 5). When the diameter is 75 mm, regardless of the particle shape, the $V_{px}(t)$ is about 0.60 ~ 1.00 times U_c, and shapes of probability density distributions are almost similar. This is because the ratio of the particle diameter to bed roughness d/k_s(= 3.26) is relatively small, and particles that collide head-on with unevenness of the bed increase in number. However, as the particle diameter increases, probability density distributions of the $V_{px}(t)$ clearly differ depending on the particle shape. When the particle shape deviates from the sphere, the peak value of the distribution and the width are small and large, respectively.

Focused on the transverse component of the instantaneous particle velocity $V_{py}(t)$ (see Fig. 6), the $V_{py}(t)$ of spherical particle is at most about ± 0.4 m/s (10 % of U_c), while that of non-spherical particles is at most about ± 0.8 m/s (20 % of U_c), regardless of the particle size. Non-spherical

particles move more three-dimensionally than spherical particles. These analytical results indicate that the motion of arbitrary shaped particles changes in the Shields number, the ratio d/k_s and the particle shape.

As described above, effects of particle shape on the distribution of the instantaneous particle velocity differ depending on the particle size. This mechanism is discussed on the fluid forces and collision forces acting on a moving particle. Fig. 7 shows the longitudinal component of time-averaged fluid force $\bar{F}_{fx}$ acting on each particle dominant in the accelerated motion. $\bar{F}_{fx}$ acting on non-spherical particles such as A075 and C075 are about 1.5 times larger than $\bar{F}_{fx}$ acting on the spherical particle (D075). As the particle size increases, $\bar{F}_{fx}$ acting on non-spherical particles such as A135, B135 and C135 are about 2.0 times larger than the $\bar{F}_{fx}$ acting on the spherical particle (D135). The larger the particle size and the more the shape deviates from the sphere, the greater fluid force and a particle acceleration.

Fig. 8 shows the longitudinal component of the collision force $|F_{cx}|$ that reduces the longitudinal component of the instantaneous particle velocity. The effect of particle shape on the mean value of $|F_{cx}|$ acting on a small particle (d = 75 mm) is very small, however, that on a large particle (d = 135 mm) differs greatly among shapes. These are two reasons. First, except for A135, the mean value of $|F_{cx}|$ also increases as the shape deviates from the sphere. Second, the large sphere (D135) rolls over the bed roughness more easily, and the collision force of D135 is lower than that of D105.

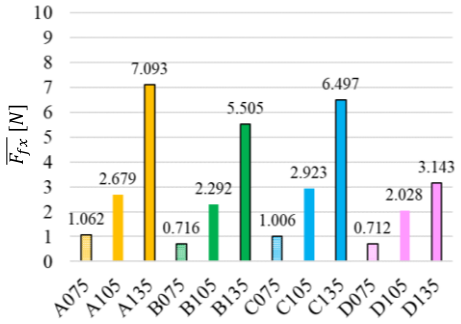

Figure. 7 The longitudinal component of the time-averaged fluid force acting on each particle. Fluid forces are averaged over the time that each particle moves between 7.5 < x < 45 m.

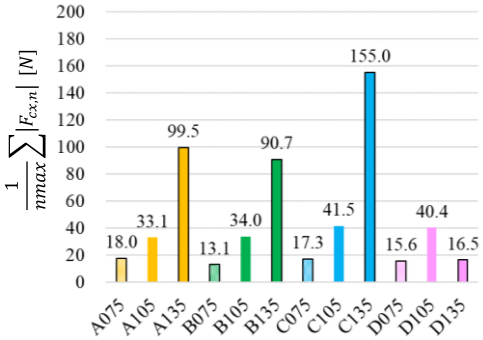

Figure. 8 The longitudinal component of the collision force acting on each particle.

4. Conclusions

Saltation motions of single particles with various volumes and sizes in a turbulent flow over a roughened bed were analyzed to clarify relationships among particle postures, instantaneous velocity, fluid forces and collision forces acting on a particle, and particle volumes and shapes. As the particle diameter increases, effects of the particle shape on its motion become significant. Non-spherical particles are transported with a large projected area in the flow direction and are accelerated by the large fluid force. However, when they hit the channel bed, they generate a large collision force and decelerates. Therefore, the instantaneous velocity of non-spherical particles varies widely. In addition, non-spherical particles have more three-dimensional motion than spherical particles.

These results would contribute to the understanding of fundamental mechanisms in gravel-bed rivers such as the momentum exchange between saltating particles and deposited particles.

Reference

[1] Krumbein (1942). *Eos, Transactions American Geophysical Union, 23(2),* 621-633. https://doi.org/10.1029/TR023i002p00621

[2] Auel et al. (2017). *Earth Surface Processes and Landforms, 42(9),* 1365-1383. https://doi.org/10.1002/esp.4128

[3] Fukuoka, et al. (2014). *Advances in Water Research, 72,*84-96. https://doi.org/10.1016/j.advwatres.2014.05.013

[4] Takakuwa and Fukuoka (2021). *J. JSCE, Ser. B1 (Hydraulic Engineering), 77(2)*, 697-702. https://doi.org/10.2208/jscejhe.77.2_I_697 (*In Japanese*).

[5] Shigemura (2004). *Master of Engineering Thesis, Hiroshima University*. (*In Japanese*).

[6] Jain et al. (2020). *Meccanica, 55*, 299-315. https://doi.org/10.1007/s11012-019-01064-6